Human Molecular Genetics, 2012, Vol. 21, No. 4 ***751–764***
doi:10.1093/hmg/ddr506
Advance Access published on November 4, 2011

Derivation of new human embryonic stem cell lines reveals rapid epigenetic progression *in vitro* that can be prevented by chemical modification of chromatin

Silvia V. Diaz Perez[1,2], Rachel Kim[3,6], Ziwei Li[1,2], Victor E. Marquez[7], Sanjeet Patel[5,6], Kathrin Plath[3,4,5,6] and Amander T. Clark[1,2,3,4,6,*]

[1]Department of Molecular Cell and Developmental Biology, [2]College of Letters and Science, [3]Jonsson Comprehensive Cancer Center, [4]Molecular Biology Institute, [5]Department of Biological Chemistry and [6]Eli and Edythe Broad Center of Regenerative Medicine and Stem Cell Research, University of California, Los Angeles, CA, USA and [7]National Cancer Institute, Frederick, MA, USA

Received October 5, 2011; Revised October 5, 2011; Accepted October 28, 2011

Human embryonic stem cells (hESCs) are pluripotent cell types derived from the inner cell mass of human blastocysts. Recent data indicate that the majority of established female XX hESC lines have undergone X chromosome inactivation (XCI) prior to differentiation, and XCI of hESCs can be either XIST-dependent (class II) or XIST-independent (class III). XCI of female hESCs precludes the use of XX hESCs as a cell-based model for examining mechanisms of XCI, and will be a challenge for studying X-linked diseases unless strategies are developed to reactivate the inactive X. In order to recover nuclei with two active X chromosomes (class I), we developed a reprogramming strategy by supplementing hESC media with the small molecules sodium butyrate and 3-deazaneplanocin A (DZNep). Our data demonstrate that successful reprogramming can occur from the XIST-dependent class II nuclear state but not class III nuclear state. To determine whether these small molecules prevent XCI, we derived six new hESC lines under normoxic conditions (UCLA1–UCLA6). We show that class I nuclei are present within the first 20 passages of hESC derivation prior to cryopreservation, and that supplementation with either sodium butyrate or DZNep preserve class I nuclei in the self-renewing state. Together, our data demonstrate that self-renewal and survival of class I nuclei are compatible with normoxic hESC derivation, and that chemical supplementation after derivation provides a strategy to prevent epigenetic progression and retain nuclei with two active X chromosomes in the self-renewing state.

INTRODUCTION

Human embryonic stem cells (hESCs) are pluripotent cells derived from pre-implantation embryos (1). These cells constitute critical cell-based tools for understanding molecular events in human embryo development, and are a source of cells for regenerative medicine. In the last 5 years, the derivation of induced pluripotent stem (IPS) cells from adult human somatic cells by reprogramming with four potent transcription factors and/or various combinations of small molecules has revolutionized pluripotent stem cell research (2–7). Human IPS (hIPS) cells have considerable advantages over hESCs, one of the most important being that hIPS cells do not originate from human embryos. However, other advantages such as generation of personalized IPS cell lines that will not be rejected by self have recently been challenged (8). Since the discovery of IPS cells, considerable effort is now invested in determining the genetic and epigenetic differences between cohorts of established hESCs and hIPS cell lines, with hESCs used as a control 'gold standard' (9–14). This begs the question: are hESCs currently maintained under conditions that warrant the title of 'gold standard', or are we unwittingly at bronze?

*To whom correspondence should be addressed at: 621, Charles E. Young Drive South, Los Angeles, CA 90095, USA. Tel: +1 3107944201; Email: clarka@ucla.edu

Gold standard mouse ESCs are identified in chimera assays where ESC derivatives would contribute to all embryonic germ layers as well as germ line cells. These chimera assays are not possible with human pluripotent stem cells. Instead, less robust assays such as teratoma formation by transplantation into immunocompromised mice are used. The mouse chimera assay is based upon the capacity of ESCs to recapitulate embryo development *in situ*; therefore, wherever possible, human pluripotent stem cells should be held to the same standard. One critical example where human pluripotent stem cells do not recapitulate embryo development involves X chromosome inactivation (XCI) in female cells. A recent study of human embryos revealed that cells of the inner cell mass (ICM) in human blastocysts contain two active X chromosomes even up to day 7 after fertilization (15). This would suggest that hESCs derived on or before day 7 from the ICM should also have two active X chromosomes. However, at a single cell level, it has been reported that hESCs in the undifferentiated state have mostly completed XCI (16–22). More importantly, there are an increasing number of reports that hESCs and hIPS cell nuclei display a non-canonical form of XCI that is XIST-independent, and is stably inherited upon differentiation (16–19,21). This heterogeneity has led to a classification system unique to pluripotent stem cells where class I nuclei exhibit two active X chromosomes (resembling XX mouse ESCs) and class II nuclei have undergone XCI with enrichment of *XIST* RNA on the inactive X, and accumulation of H3K27me3 (histone H3 lysine 27 trimethylation) (23,24). Class III nuclei in contrast are XCI, yet are negative for *XIST* and show no enrichment of H3K27me3 on the inactive X.

The importance of documenting class I, II and III epigenetic status of individual hESC and hIPS cell nuclei under standard culture conditions is critical for analysis of X-linked disease models, as well as for studies aimed at understanding mechanisms of XCI. Furthermore, understanding the timing of XCI can facilitate a more accurate understanding of the origin of hESCs relative to other *in vitro* pluripotent counterparts, for example murine epiblast stem cells (EpiSCs), which also exhibit XCI in culture due to their origin from epiblast (reviewed in 25). With regard to differentiation, one study has suggested that generation of embryoid bodies (EBs) from hESC lines composed of predominantly class III nuclei is poor and questions whether class III hESC lines are pluripotent (17). However, poor differentiation potential of class III cells and capacity to generate teratomas remain to be independently established. Taken together, due to the importance of generating a cell type that recapitulates the stage at which hESCs are derived, and the capacity for maximal differentiation potential *in vitro*, there is considerable interest in developing strategies to preserve or acquire hESCs in the class I nuclear state. Towards this end, derivation of new hESC lines in hypoxia has been shown to enrich for class I nuclei (26). However, this effect is not universally effective (26). Human ESC and hIPS cell lines that have already undergone XCI can be reprogrammed to class I with introduction of *octamer binding transcription factor 4* (*Oct4*), *Kruppel-like factor 4* (*Klf4*) and *Klf2* transgenes and growth in mouse ESC media (22,27). However, stable modification is required for this technique to be successful. The histone deacetylase inhibitor sodium butyrate (B) has been used to reprogram the H9 hESC line (28). However, it is unclear whether this effect is also applicable to other hESC lines.

In the current study, we chose to evaluate a new non-integrative method of reprogramming using the small molecule 3-deazaneplanocin A (DZNep) to acquire nuclei in the class I state. DZNep was originally shown to deplete cellular levels of enhancer of zeste homolog2 (EZH2) and therefore removal of H3K27me3 from the genome (29–31). More recent studies indicate that DZNep has a global effect on chromatin, repressing a variety of both active and repressive histone marks in cancer cells by mechanisms that are unclear (32). Given that H3K27me3 accumulation is one of the critical components of class II XCI, our hypothesis is that culture of hESCs with DZNep would facilitate the propagation of class I nuclei from class II. This study represents a comprehensive evaluation of the hESC epigenetic status at a single-cell level in six independently derived hESC lines in order to develop a strategy to sustain hESC nuclei in the class I state.

RESULTS

Undifferentiated hESC lines are heterogeneous

In order to examine the XCI status of undifferentiated HSF-6 (p51) female hESCs in our laboratory, we co-stained OCT4 with H3K27me3 (Fig. 1A–D). OCT4 protein was localized to the nucleus of all cells within a given colony; however, signal intensity varied from nucleus to nucleus (Fig. 1B, arrows indicate a bright and dim nucleus). Staining with H3K27me3 revealed small focal dot-like structures (arrows indicating two different examples) in some but not all OCT4-positive nuclei (Fig. 1B–D). Given that OCT4 protein levels exhibit phasic cycling in undifferentiated ESCs (33), and increased *XIST* RNA have been correlated with lower *OCT4* RNA levels in undifferentiated hESCs (18), we next sought to determine whether H3K27me3 foci (Fig. 1E and G) correlated with either OCT4 bright (Br) or OCT4 dim (Di) nuclei (Fig. 1F and H). We counted nuclei that contained H3K27me3 foci (K27+) as well as nuclei without H3K27me3 foci (K27−) and evaluated OCT4 protein levels within the two populations. In co-staining OCT4 with H3K27me3, we also noticed potential OCT4 foci only in nuclei with enriched focal dot of H3K27me3 (Fig. 1E and F, arrow). However, immunofluorescence using OCT4 alone revealed no OCT4 foci (Fig. 1I and J), indicating that the 'dot' in the OCT4 channel when co-stained with H3K27me3 is a technical artifact. Despite this, we could still analyze nuclei that contained a global bright (Br) or globally dim (Di) expression of OCT4, and found no correlation between OCT4 protein levels and the presence or absence of an H3K27me3 focal dot (Fig. 1K).

In order to confirm that H3K27me3 was enriched on an X chromosome, we combined H3K27me3 staining with X chromosome fluorescence *in situ* hybridization (FISH) (Fig. 1L–Q). Our data show that all HSF-6 hESC nuclei in this analysis contained two X chromosomes (Fig. 1L and O). Co-staining with H3K27me3 revealed that some of the X chromosomes exhibit no H3K27me3 foci (Fig. 1M and N). In contrast, other nuclei show specific enrichment with a

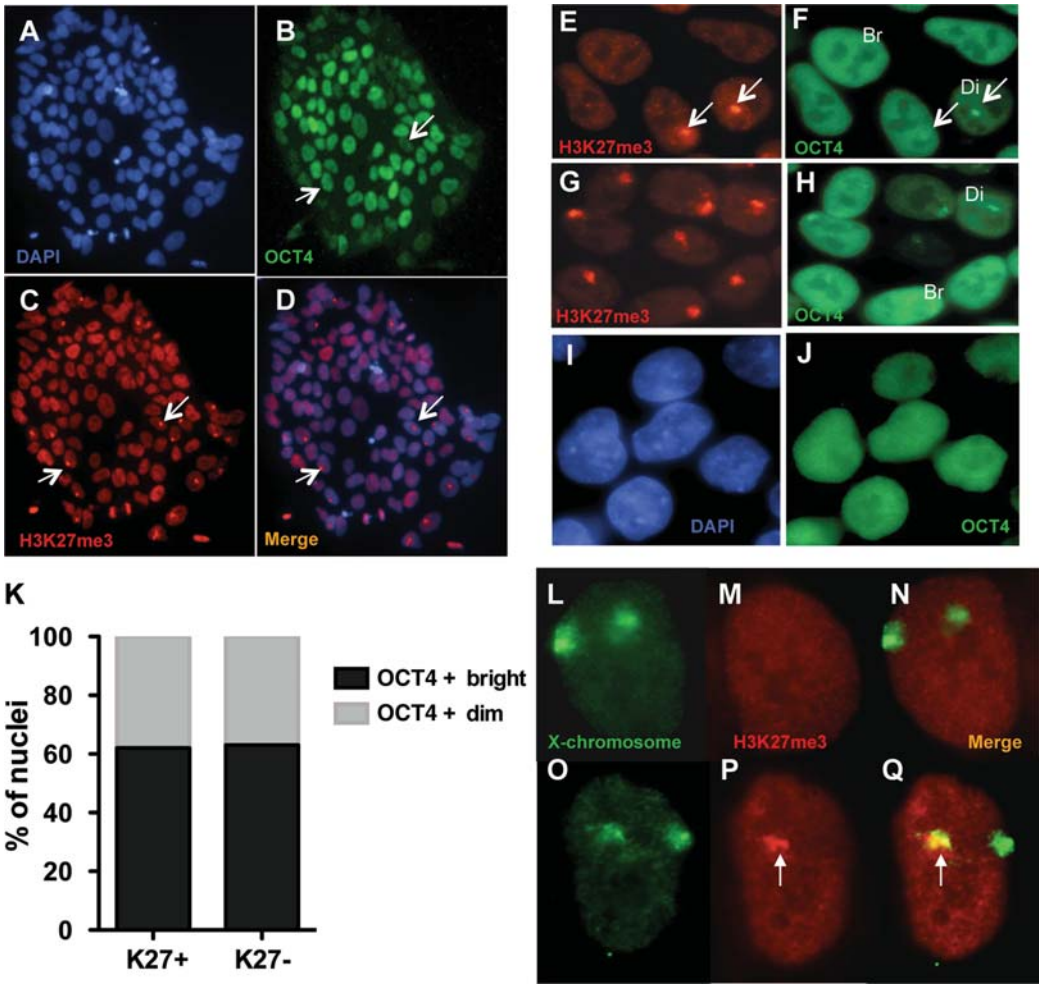

Figure 1. H3K27m3 and OCT4 expression in undifferentiated hESCs. Shown are representative immunofluorescence images of the HSF-6 hESC line at passage 51, (**A**) DAPI, (**B**) OCT4, (**C**) H3K27me3 (arrow indicating focal dot in some nuclei), (**D**) Merger of (A) and (C). (**E** and **G**) H3K27me3, (**F**, **H** and **J**) OCT4, with arrows indicating bright (Br) or dim (Di) OCT4-positive nuclei, (**I**) DAPI. (**K**) OCT4-positive ($n = 247$, Br and Di) nuclei were counted and results are shown as percentage of bright or dim nuclei with and without H3K27me3 foci. (**L** and **O**) X chromosome paint, (**M** and **P**) H3K27me3, (**N**) Merger of (L) and (M) and (**Q**) Merger of (O) and (P).

single H3K27me3 focal dot that correlates with one of the X chromosomes (Fig. 1P and Q, arrow). This nucleus is therefore considered to have undergone XCI. Taken together, these data support work from other laboratories establishing that lines of hESCs are heterogeneous at any given time with regard to the XCI status, and provide new data that H3K27me3 enrichment on the X does not correlate with the intensity of OCT4 protein expression in the nucleus.

Human ESC lines undergo unidirectional progression to class III

In order to determine the identity of nuclei without H3K27me3 foci, we generated sublines of the HSF-6 and H9 parental lines of female hESCs (Supplementary Material, Table S1). In HSF-6 and H9 hESC lines at the start of the experiment, the percentage of nuclei with a single H3K27me3 focal dot was characterized as 40% at passage 57 (HSF-6) and 36% at passage 37 (H9). Ten colonies of HSF-6 were picked and analyzed at passage 61. Our data show that the majority of HSF-6 sublines at passage 61 were similar to the original line at passage 57. However, we identified three sublines where 95% of nuclei exhibited H3K27me3 foci (called HSF-6 (7), HSF-6 (8) and HSF-6 (10)). Interestingly, at the same time we established four HSF-6 sublines from single cells using the Rho kinase (ROCK) inhibitor, and all sublines generated from single cells exhibited zero nuclei with H3K27me3 foci after seven passages. Ten sublines were also generated from the H9 hESC line by colony-picking and analyzed at passage 41. We found that unlike HSF-6, most picked H9 sublines contained no H3K27me3 foci, and the parental H9 line, which was also analyzed at passage 41, also did not exhibit any nuclei with H3K27me3 foci. Taken together, these experiments demonstrate that regular culturing, as well as the generation of sublines from single cells with ROCK inhibitor, can result in rapid loss of cells with H3K27me3 coating on the X chromosome.

In order to determine whether the presence or absence of H3K27me3 foci is retained during differentiation, we evaluated HSF-6 (7), HSF-6 (8) and HSF-6 (10) (Fig. 2A), and

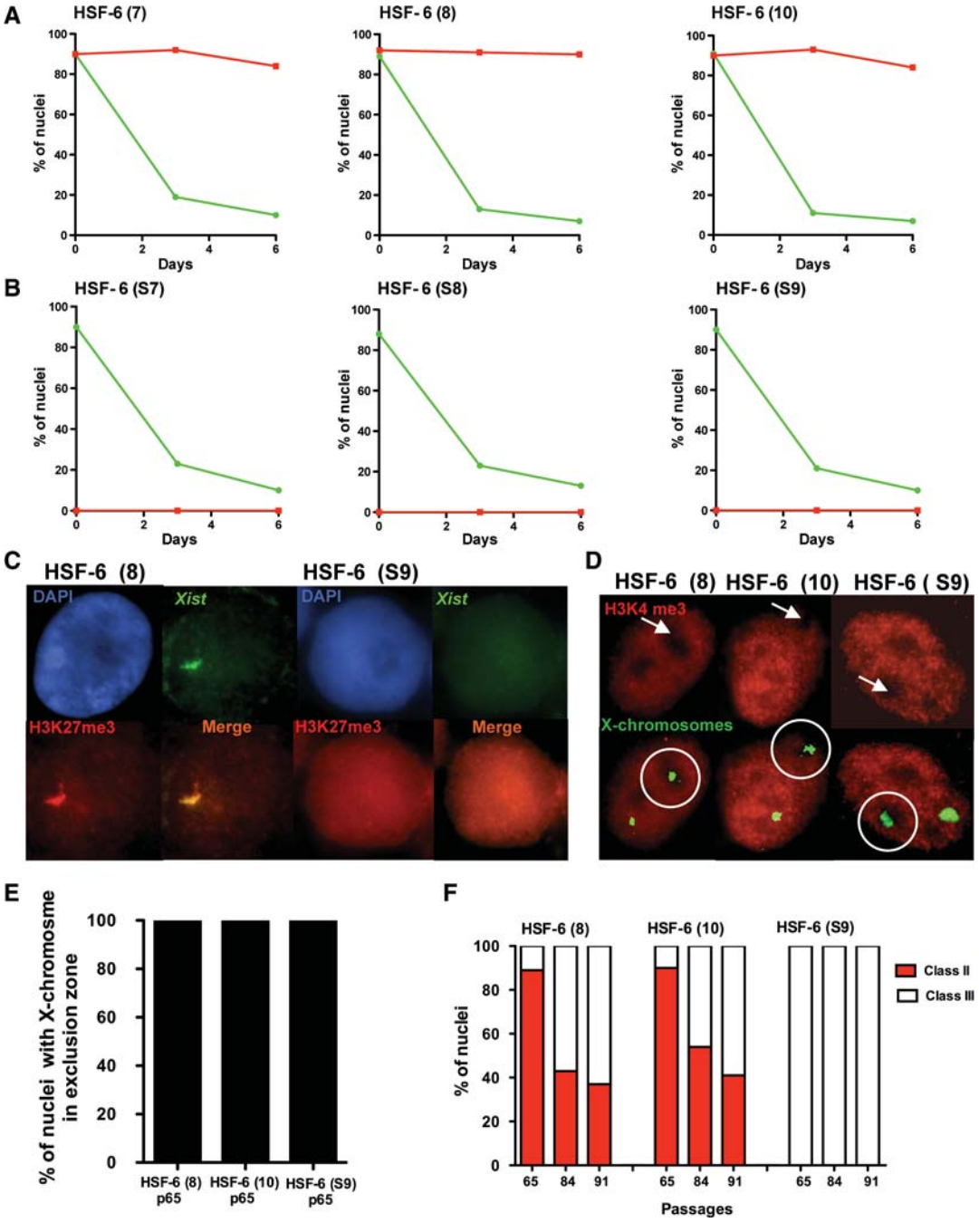

Figure 2. Epigenetic status of the X chromosome with differentiation or serial passaging. (**A**) Six-day differentiation of HSF-6 (7), HSF-6 (8) and HSF-6 (10). OCT4+ and H3K27me3+ nuclei were counted at days 0, 3 and 6 of differentiation in each subline ($n = 200$ nuclei at each time point in each subline). (**B**) HSF-6 (S7), HSF-6 (S8), HSF-6 (S9) were differentiated in the same conditions as above ($n = 200$ nuclei for each data point). (**C**) *XIST* RNA FISH combined with immunostaining for H3K27me3. HSF-6 (8) ($n = 80/80$) nuclei exhibited co-localization of XIST with H3K27me3. HSF-6 (S9) ($n = 120/120$) nuclei did not exhibit any *XIST* signal. (**D**) X chromosome FISH combined with immunostaining for H3K4me3 (H3K4me3/X FISH). White and green arrows show nuclear exclusion zones. The white circles show the localization of one X chromosome in one exclusion zone. (**E**) Quantification of data in (D) ($n = 10$) for each subline. (**F**) Transition of class II to class III is unidirectional. Class II and class III nuclei were evaluated on duplicate cover slips collected at passages 65, 84 and 91 in HSF-6 (8), HSF-6 (10) and HSF-6 (S9). Class II nuclei were evaluated by scoring H3K27me3 foci ($n = 200$); XCI was identified using H3K4me3/X FISH ($n = 10$). Class III = n(H3K4me3/X FISH) – n(H3K27me3).

HSF-6 (S7), HSF-6 (S8) and HSF-6 (S9) (Fig. 2B). The percentage of OCT4-positive nuclei was quantified at all time points after the induction of differentiation in order to evaluate the loss of pluripotency. All sublines were differentiated for 6 days and evaluated at days 0, 3 and 6 of differentiation. Our data show that upon differentiation and loss of OCT4, H3K27me3 foci are maintained during differentiation in HSF-6 (7), HSF-6 (8) and HSF-6 (10) sublines (Fig. 2A).

Similarly, sublines that exhibited zero H3K27me3 foci, namely HSF-6 (S7), HSF-6 (S8) and HSF-6 (S9) (Fig. 2B), did not acquire H3K27me3 foci upon differentiation. Together these data suggest that HSF-6 (7), (8) and (10) are of class II, and HSF-6 (S7), (S8) and (S9) are of class III, and provide *in vitro* evidence refuting the hypothesis that class III nuclei *in vitro* are unable to differentiate.

In order to confirm the class II and class III status of HSF-6 (8) and HSF-6 (S9), respectively, we performed *XIST* RNA FISH (Fig. 2C). Our data show that H3K27me3 nuclear foci in HSF-6 (8) correlate with XIST RNA coating, confirming that HSF-6 (8) is in a class II state as defined by Silva *et al*. (17). We also determined that HSF-6 (S9) nuclei are negative for *XIST* (Fig. 2C). Combined with the differentiation data above, this result demonstrates that HSF-6 (8) is in a class II state and HSF-6 (S9) is in a class III state. In order to prove class III status, we performed a modification of the nuclear Cot-1 RNA exclusion assay using Cot-1/X FISH (17). We reasoned that as Cot1 is used to indicate active transcription, we could replace Cot1 RNA FISH with immunofluorescence for the histone mark H3K4me3 (histone H3 lysine 4 trimethylation), which is localized to active chromatin (Supplementary Material, Figure S1). Application of the H3K4me3/X FISH technique to HSF-6 (8), HSF-6 (10) and HSF-6 (S9) revealed large nuclear exclusion zones following H3K4me3 staining in all nuclei, with one X chromosome located in one exclusion zone in each nucleus (Fig. 2D, white arrows and white circles). Quantification of individual nuclei in the three sublines by this technique revealed that 100% of nuclei had undergone XCI (Fig. 2E). However, given that the HSF-6 (S9) subline has zero foci of H3K27me3 and was also negative for *XIST* RNA, it can be confirmed that HSF-6 (S9) is composed of 100% class III nuclei.

To determine whether transition from class II to class III is unidirectional, we followed HSF-6 (8), HSF-6 (10) and HSF-6 (S9) for 30 consecutive passages (passages 61–91) (Fig. 2F). Analysis of class II nuclei by H3K27me3 and class I nuclei by H3K4me3/X FISH was performed at passages 65, 84 and 91 (Fig. 2F). At each passage, we collected replicate samples on cover slips and performed H3K27me3 staining on one slide, and H3K4me3/X FISH on a duplicate slide. This enabled us to evaluate both class II nuclei using H3K27me3, and analysis of total number of nuclei that have undergone XCI by H3K4me3/X FISH. Class II nuclei were first quantified by scoring nuclei with and without H2K27me3 foci. XCI was next evaluated by analysis of X chromosome localization to an exclusion zone using H3K4me3/X FISH. Given that 100% of nuclei exhibited XCI by H3K4me3/X FISH at all passages tested, we can deduce that by passage 91, $<40\%$ of nuclei in HSF-6 (8) or HSF-6 (10) are in a class II state, with $>60\%$ corresponding to class III. In contrast, the class III subline HSF-6 (S9) remained stable in the class III state (Fig. 2F). Finally, in order to address the question of pluripotency of the class III hESC line, we performed teratoma analysis of the eight putative class III lines and sublines (four from HSF-6 and four from H9) (Supplementary Material, Figure S2). This result demonstrates that all eight class III lines and/or sublines are capable of teratoma formation *in vivo* with evidence of ectoderm, mesoderm and endoderm formation. This result strongly refutes the hypothesis that hESC lines consisting of class III nuclei are not pluripotent.

Addition of butyrate or butyrate and DZNep to class II and class III sublines results in reprogramming of class II to class I

Previous studies have shown that sodium butyrate (B) can reprogram H9 female hESCs to class I. However, it is not known whether B acted on class II or class III nuclei to achieve reprogramming, or whether this effect can be repeated with other hESC lines. Using the sublines described above, we established an experiment in which HSF-6 (8), HSF-6 (10) and HSF-6 (S9) were cultured in either control (C) conditions for 22 consecutive passages, or treated with the small molecule B for 22 consecutive passages, or B for 5 passages, followed by 17 passages in B plus DZNep (B + D) (Fig. 3A). We first performed a dose–response curve to identify the optimal dose of D to use in combination with B. Previous studies have used 5 μM DZNep to promote global loss of H3K27me3; however, this dose also induces apoptosis (31,32). Therefore, we tested 5, 1, 0.1 and 0.05 μM for an effect on class II nuclei together with B in a 5-day culture period. We determined that 5 and 1 μM were highly toxic to the hESCs during the short culture period (data not shown). However, 0.1 and 0.05 μM resulted in no obvious lethality. Furthermore, addition of 0.1 and 0.05 μM D to B-treated cultures resulted in a 28 and 13% drop in class II nuclei, respectively, compared with B alone. Therefore, 0.1 μM was chosen as the dose of DZNep for all future experiments. At passage 92, histones from HSF-6 (8) and HSF-6 (S9) with and without B and B + D were purified and analyzed for H3K27me3 and H3K4me3 by immunobloting (Fig. 3B). This result shows that at the dose of chemicals used in the current study, we did not overtly affect the global amount of H3K27me3 or H3K4me3 relative to control H3 in the HSF-6 (8) or HSF-6 (10) hESC lines; however, we did observe a very mild depletion of H3K27me3 in B and B + D-treated cultures of HSF-6 (9) relative to C (Fig. 3B).

In order to determine whether the chemicals had any effect on H3K27me3 coating of the X chromosome, we performed H3K27me3 staining at passages 84 and 91 (Fig. 3C and D), and quantified percentage of class II nuclei by scoring for the presence of H3K27me3 foci. Treatment with either B or B + D decreased the percentage of class II nuclei relative to control at both passages, but had no effect on the HSF-6 (S9) class III subline, which remained negative. In order to determine whether the loss of class II nuclei in HSF-6 (8) and (10) was due to the acquisition of class I nuclei, we performed the nuclear exclusion assay of H3K4me3/X FISH in B + D-treated cultures relative to control (Fig. 3E and F). Using this assay, our data show that treatment with B + D resulted in the emergence of 30% class I nuclei in HSF-6 (8) and HSF-6 (10). Zero class I nuclei were identified in HSF-6 (S9) class III treated with B + D (Fig. 3E). Together, these data demonstrate that class III nuclei are non-reprogrammable in B + D with regard to the movement of an entire X chromosome out of the exclusion zone. To evaluate self-renewal in B + D conditions, we stained hESC lines

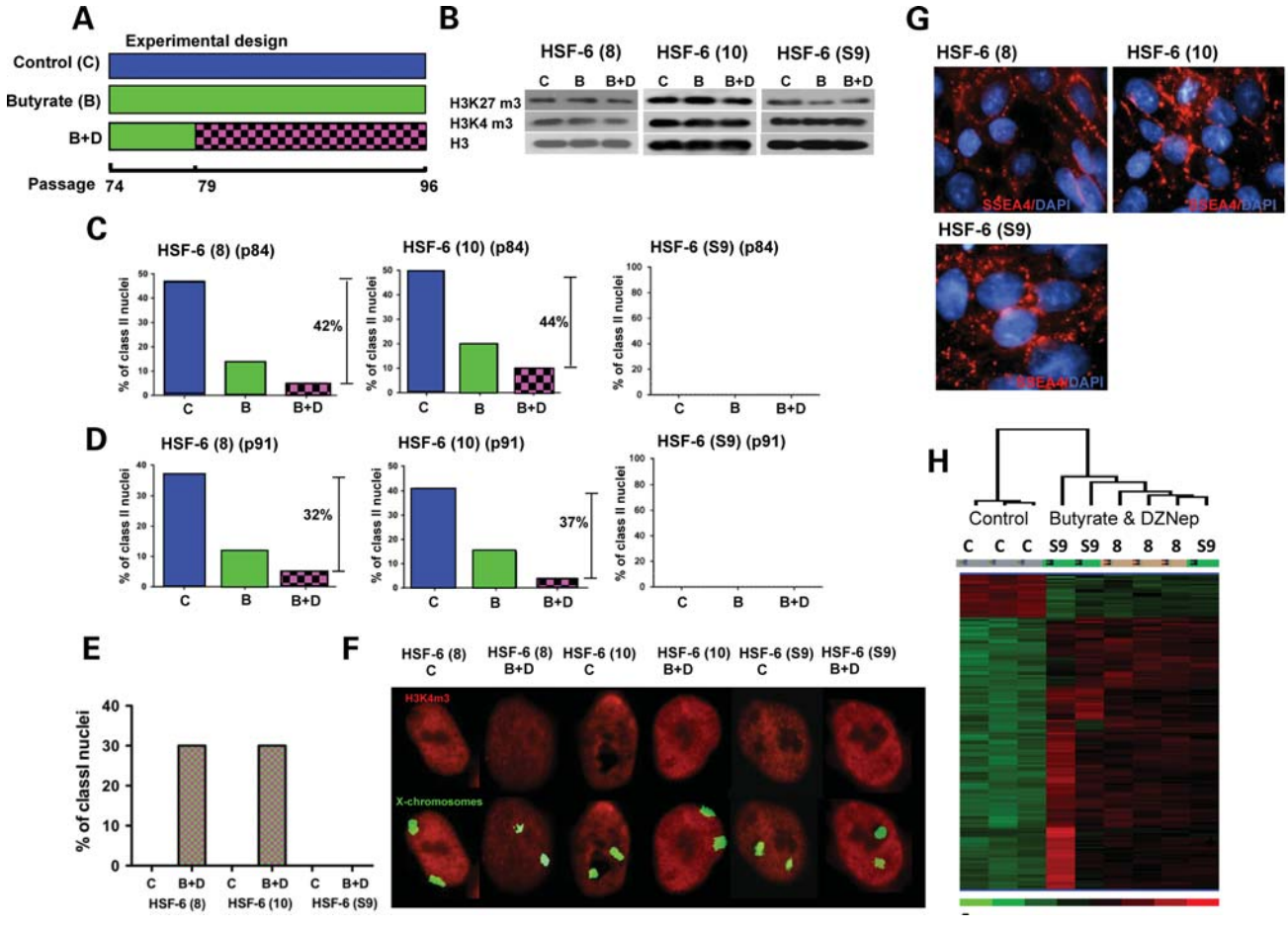

Figure 3. Reprogramming of class II hESCs to class I. (**A**) Experimental design for analysis of HSF-6 (8), HSF-6 (10) and HSF-6 (S9) over 22 passages. (**B**) Western blot of purified histones blotted for H3K27me3, H3K4me3 and the loading control histone H3 in HSF-6 (8), HSF-6 (10) and HSF-6 (S9). (**C**) Class II analysis at passage 84 by staining for H3K27me3 and scoring foci. Numbers in parentheses indicate total number of nuclei evaluated. For HSF-6 (8): C (272), B (352) and B + D (439). For HSF-6 (10): C (336), B (402) and B + D (403). For HSF-6 (S9): C (330), B (342) and B + D (362). (**D**) Effect of B and B + D at passage 91: HSF-6 (8): C (310), B (322) and B + D (453). HSF-6 (10): C (310), B (322), B + D (453). HSF-6 (10): C (334), B (354), B + D (491). HSF-6 (S9): C (185), B (225), B + D (246). (**E**) Loss of class II nuclei was due to an increase in the proportion of class I nuclei in B + D as determined by H3K4me3/X FISH at passage 91 ($n = 10$ each sample). (**F**) Representative images of H3K4me3/X FISH at passage 91. (**G**) SSEA4, immunoflourescence of B + D-treated cell lines at passage 96. (**H**) Heat map of microarray comparing HSF-6 (8) C- and HSF-6 (8) B + D-treated cultures ($P < 0.01$, $\geq$1.5-fold difference). HSF-6 (S9) B + D microarray samples cluster with HSF-6 (8) B + D samples.

with SSEA4 using immunofluorescence, and found robust surface expression (Fig. 3G).

Finally, in order to determine how B + D affects global gene expression, we performed microarray analysis in triplicate in the HSF-6 (8) C- and HSF-6 (8) B + D-treated cultures (Fig. 3H). We also evaluated HSF-6 (S9) B + D in triplicate and identified no statistically significant changes in gene expression in HSF-6 (S9) B + D- compared with HSF-6 (8) B + D-treated cultures. This suggests that global transcriptional differences are more strongly modulated by presence or absence of B + D and not the percentage of class I, II or III nuclei. When comparing microarrays of HSF-6 (8) C- with HSF-6 (8) B + D-treated cells, we identified 170 differentially expressed genes with independent accession numbers (Fig. 3H and Supplementary Material, Table S2). The heat map demonstrates that the majority of differentially expressed genes were increased >1.5-fold in B + D-treated cultures compared with C. Of the 170 differentially expressed gene accession numbers, 12 map to the X chromosome including, *kelch-like 15* (*KLHL15*), *motile sperm domain containing 1* (*MOSPD1*), *suppressor of hairy wing homolog 3* (*SUHW3*), *male-specific lethal 3-like 1* (*MSL3L1*), *thymosin-like 8* (*TMSL8*), *dystrophin* (*DMD*), *four and a half LIM domains 1* (*FHL1*) (corresponding to two independent accession numbers), *SLIT and NTRK-like family, member 4* (*SLITRK4*), *monoamine oxidase A 9* (*MAOA*), *melanoma antigen family A2* (*MAGEA2*) and *transcription elongation factor A (SII)-like 2* (*TCEAL2*). Thus, we propose that B and D are acting in two ways on undifferentiated hESCs. These are: (i) to reverse the epigenetic state of the X chromosome in class II nuclei by moving a percentage of X chromosomes out of the H3K4me3 exclusion zone, and (ii) to regulate gene expression of a small number of genes genome-wide including genes on the X chromosome.

Table 1. Embryo characteristics and resulting hESC lines derived from the consented embryos

Embryo number	Stage donated	Quality of embryos	Date of freezing of embryos	Date of thawing of embryos	New hESC name	Karyo	% class I nuclei by H3K4/X FISH (p, passage)
AN043	Frozen	ND	10/08/05	08/06/09	UCLA1	46, XX	58 (p1); 65 (p12)
AN044	Frozen	ND	10/08/05	08/06/09	UCLA2	46, XY	ND
AN050	Frozen	ND	10/08/05	08/24/09	UCLA3	46, XX	100 (p1); 100 (p10); 100(p19)
AN089	Frozen	3ABA	12/04/06	03/03/10	UCLA4	46, XX	95 (p20)
AN104	Frozen	ND	1/15/06	04/04/10	UCLA5	46, XX	77 (p19)
AN110	Frozen	4AA	6/22/04	04/21/10	UCLA6	46, XY	ND

ND, not determined; Karyo, karyotype.

New hESC lines exhibit a range of epigenetic identities, with class I nuclei identified in all early passage female hESC lines derived under normoxic conditions

Given that the established female hESC lines in our laboratory cultured under standard normoxic conditions did not exhibit any evidence of class I nuclei (as defined using the H3K4me3 nuclear exclusion assay), we derived six new hESC lines from frozen blastocysts under normoxic conditions, which we called UCLA1–UCLA6 in order to determine whether class I nuclei could be observed during the initial derivation and establishment of hESC lines (Table 1). The day of derivation from human blastocysts was between day 6 and day 7 after fertilization. In this cohort of hESC lines, we determined that all lines were karyotypically normal, expressed the surface makers TRA-1-81 and SSEA4 (Supplementary Material, Figure S3) and generated teratomas when transplanted into SCID-Beige mice (Supplementary Material, Figure S4). Four of the six lines were female, and thus informative for our analysis. Class I nuclei were evaluated in the four female lines by H3K4me3/X FISH during the derivation process up to passage 20 (Table 1). These experiments were performed on cells during the continuous process of derivation and line establishment, and before cryopreservation. Our data show that class I nuclei are identified in all four lines of female hESCs derived under normoxic conditions prior to passage 20; however, the proportion of class I nuclei are dynamic between independently derived hESC lines as well as at different passages within the same line. For example, one line (UCLA3) exhibited 100% class I nuclei over three independent passages. In contrast, UCLA1 ranged from 58 to 65% class I nuclei. It should be noted that UCLA1 and UCLA3 embryos were donated from the same parents and frozen in the same *in vitro* fertilization (IVF) cycle, thus sharing a genetic heritage. With regard to the other two genetically unrelated hESC lines, UCLA4 exhibited 95% class I nuclei at passage 20, and UCLA5 exhibited 77% class I nuclei at passage 19. This result indicates that class I nuclei are observed very early during the process of hESC derivation and line establishment under normoxic conditions in all female hESC lines; however, the self-renewal and/or survival of class I nuclei seems to be line-dependent.

Butyrate and DZNep can promote self-renewal of class I nuclei by preventing progression to class II

In order to confirm that UCLA3, during hESC derivation, was of class I, we induced differentiation and performed H3K27me3 staining at days 0, 5 and 12 (Fig. 4A). Our data show that class II nuclei are acquired when UCLA3 is induced to differentiate (Fig. 4A and B). Next, we cultured UCLA3 in the presence of B, D and B + D for four passages (28 days), starting from passage 20, and evaluated the proportion of class I and III nuclei by H3K4me3/X FISH, and class II nuclei by H3K27me3 at the end of passage 24 (Fig. 4C and D). Zero nuclei were identified as being in a class II state (images of H3K27me3 nuclei not shown), and instead only class I and class III nuclei were observed after the 28-day treatment. Morphological analysis of nuclei stained with H3K4me3 revealed that the addition of small molecules did not affect the generation and/or maintenance of nuclear exclusion zones in UCLA3 (Fig. 4C). However, in >80% of nuclei, both X chromosomes were found outside the nuclear exclusion zones, and are therefore categorized as class I (Fig. 4D). This result suggests that B and D do not promote the loss of class I in new hESC lines after 1 month of continuous culture.

Next, we evaluated UCLA1 at passage 24 after four passages in C, B, D or B + D (Fig. 4E). Treatment from passages 20–24 caused an increase in the proportion of class I nuclei compared with C-untreated cultures, with a specific loss in cells from the class II fraction and an increase in class I and class III (Fig. 4E and F). This result is consistent with an effect of the chemicals specifically on class II nuclei. In order to evaluate self-renewal of treated and control cells, we stained UCLA1 at passage 24 with TRA-1-81 and SSEA4 and found that treated cell lines are indistinguishable from control cells and to each other, thus confirming data from Figure 3G that chemical treatment does not promote loss of self-renewal markers.

Given that the effects of the chemicals were informative, yet subtle after only four passages, we tested UCLA4 for 14 passages also starting at passage 20. Similar to UCLA3, UCLA4 at passage 20 was composed of 95% class I and 5% class III nuclei (Fig. 4H). No class II nuclei were observed at passage 20. Samples were analyzed at passages 24, 30 and 34 in C, B, D, or B + D conditions. Our data show that by passage 34, UCLA4 had progressed to <5% class I nuclei in C conditions. In contrast, treatment with B, D and B + D during the 14 passages resulted in sustained percentages of class I nuclei >70% in the case of B alone, 70–80% in the case of D alone and 70–90% in the case of B + D over sequential passaging (Fig. 4H). These data suggest that either B or D or both can sustain the majority of nuclei in a class I state for more than 10 passages.

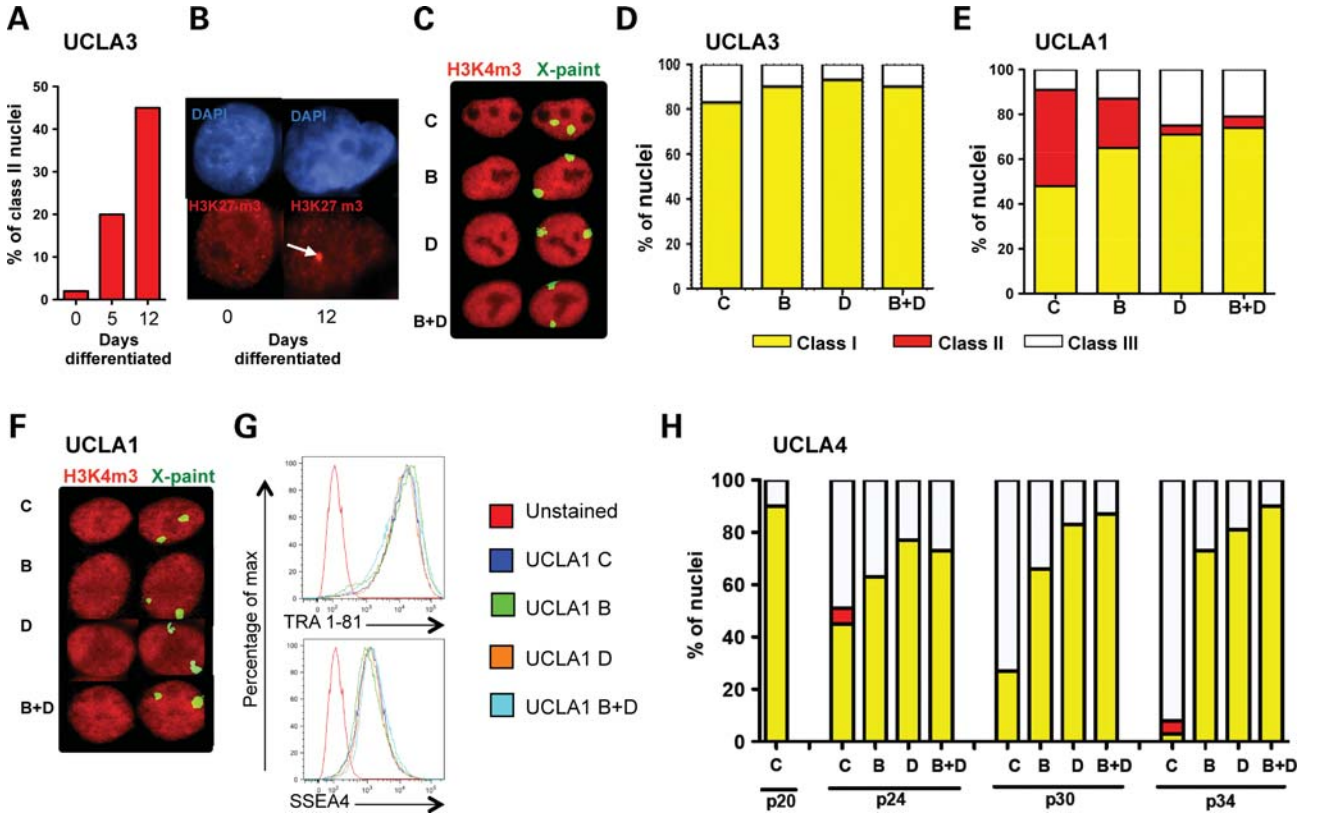

Figure 4. Reprogramming of new hESC lines. (**A** and **B**) Differentiation of UCLA3 for 12 days. (A) Quantification of H3K27me3 foci (class II) at day 0 ($n = 599$), day 5 ($n = 259$) and day 12 ($n = 259$). (B) Representative image of acquired H3K27me3 foci at day 12 (white arrow) relative to undifferentiated (day 0). (**C**) H3K4me3/X FISH at passage 24 to identify class I cells. Total nuclei counted in each condition include C ($n = 30$), B ($n = 30$), D ($n = 30$) and B + D ($n = 30$). (**D**) H3K27me3 staining was performed on a duplicate cover slip to identify class II nuclei. Total nuclei counted include C (572), B (476), D (507) and B + D (543). Data are shown as a composite of class I, II and III nuclei at passage 24 (note $n = 0$, class II nuclei). (**E**) UCLA1 after four passages in C, B, D, B + D, and quantification of class I, class II and class III nuclei. Nuclei counted using H3K27me3: C (466), B (532), D (596) and B + D (585). Nuclei counted using H3K4me3/X FISH ($n = 31$ each condition). (**F**) Images of H3K4me3/X FISH UCLA1 nuclei in each condition. (**G**) Flow plot showing TRA-1−81 and SSEA4 expression relative to secondary only control (unstained). (**H**) Class I, II and III nuclei at passages (p) 20, 24, 30 and 34 in UCLA4 as indicated. Calculations: class I = % nuclei with neither X chromosome in exclusion zone; class II = % nuclei with H3K27me3 foci; class III = % nuclei with one X chromosome in exclusion zone − % class II nuclei.

Finally, in order to address the stability of class I, II and III nuclei in the four female hESC lines after cryopreservation, we created a frozen bank of hESC lines during the course of derivation with UCLA1 cryopreserved at passage 8, UCLA3 at passage 9, UCLA4 at passage 9 and UCLA5 cryopreserved at passage 20 after plating blastocysts on mouse embryonic fibrolasts (MEFs). As previously shown under control normoxic conditions without an intervening cryopreservation event, all female cell lines exhibited some class I cells at least to passage 20, with UCLA3 and UCLA4 exhibiting the most stable self-renewal and survival of class I nuclei at 95–100% (Fig. 4 and Table 1). The four female hESC lines were thawed under normoxic conditions and each line was cultured simultaneously in the same media, on the same MEFs for more than 10 passages splitting every 7 days with collagenase. UCLA1 was analyzed at passage 24, UCLA3 at passage 25, UCLA4 at passage 20 and UCLA5 at passage 31 (Fig. 5). First, we performed H3K27me3 staining, which was negative in all hESC lines, indicating that the hESC lines after cryopreservation were composed entirely of class I or class III cells (data not shown). On duplicate cover slips, we next performed a three-color FISH to examine *XIST*, *ATRX*, which is an X-linked gene that is monoallelic in cells that have undergone XCI, such as female fibroblasts (Fig. 5A), and *UTX*, which is an X-linked gene that escapes X inactivation and is therefore used as an alternative to X chromosome paint (Fig. 5A–E). In contrast to female fibroblasts, we determined that *XIST* (pink clouds) were absent in all hESC nuclei (Fig. 5B–E), correlating with the absence of H3K27me3. With regard to *ARTX*, our results demonstrate that UCLA1, UCLA3 and UCLA5 are now composed entirely of class III nuclei at passages 24, 25 and 31, respectively, with only a single focal dot of *ATRX* in each nucleus. UCLA4 was the only cell line that exhibited a significant fraction of class I nuclei after cryopreservation, thawing and sequential passaging to passage 20 as observed by a biallelic expression of *ATRX*; however, a substantial fraction of UCLA4 nuclei in the same experiment had also progressed to class III (Fig. 5F).

DISCUSSION

Human ESCs are the gold standard to which hIPS cells are measured. Previous investigators have documented the

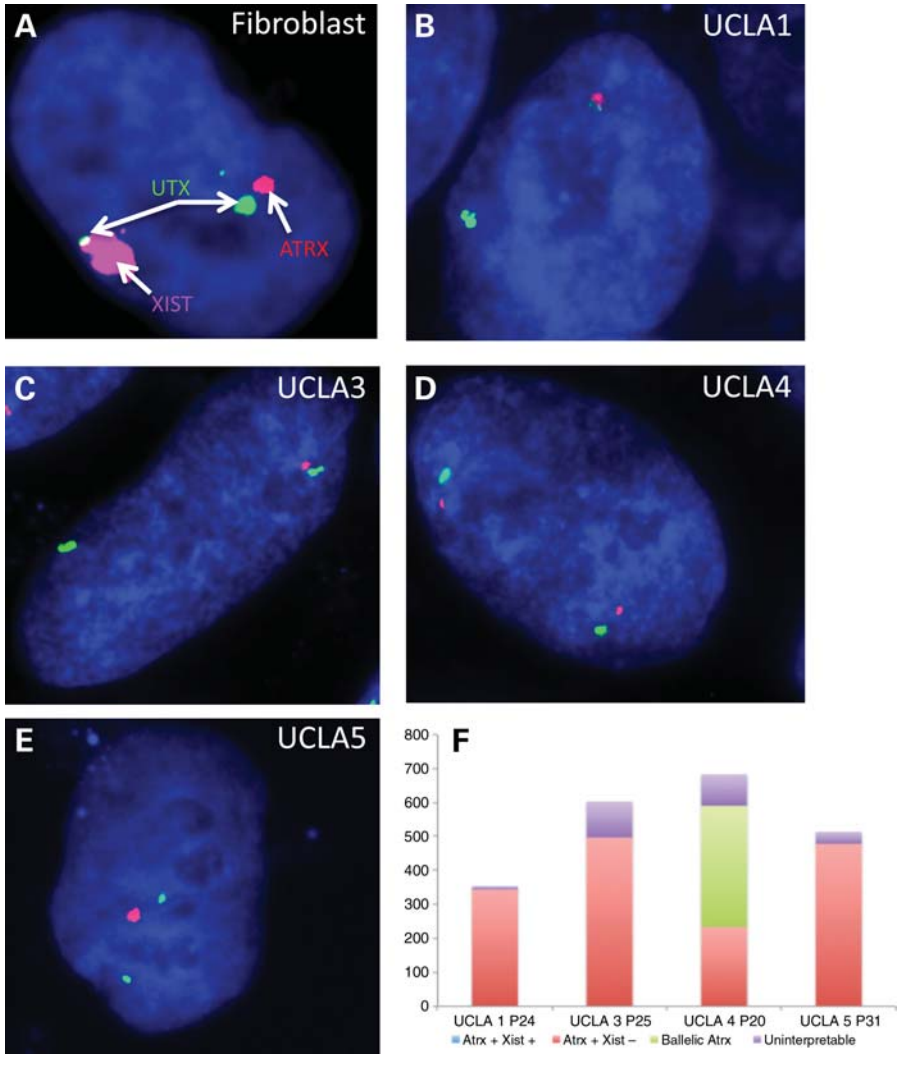

Figure 5. Cryopreservation increases incidence of class III in new hESC lines. Three-color FISH for *XIST* (pink), *UTX* (green) and *ATRX* (red) was performed on (**A**) female NHDF 17914 fibroblasts, (**B**) UCLA1 at passage (p) (p24), (**C**) UCLA3 at p25, (**D**) UCLA4 at p20, (**E**) UCLA5 at p31. (**F**) Interphase nuclei were analyzed from at least five randomly selected colonies in each hESC line, and the total sum of nuclei in each category are shown. *Y*-axis corresponds to total number of nuclei counted.

epigenetic state of the X chromosome in hESCs after line establishment and on cells that have been exposed to at least one cryopreservation event. The general consensus is that established lines of hESCs have undergone XCI, and this result is often used as epigenetic evidence (together with culture conditions) that hESCs are more closely related to murine EpiSCs, which also exhibit XCI (reviewed in 25). EpiSCs are derived from dissected epiblasts at either day 5.75 post-coitum (34), or egg cylinder stage embryos at day 5.5 post-coitum (35). In the mouse, this stage is when major changes to the embryo are underway, including the loss of the zonapellucida, implantation in the uterine epithelium and specialization of the extra embryonic lineages. In our study, human embryos were derived from blastocysts at days 6–7 post-fertilization where the zonapellucida was still mostly encapsulating a simple blastocyst (Supplementary Material, Figure S5). This stage of human development has been elegantly analyzed by Okamoto *et al*. (15), which revealed that the majority of blastomeres at day 7 exhibit biallelic X-linked gene expression, and no enrichment of H3K27me3 on an X chromosome. In our study, we show that the new UCLA hESC lines derived from days 6–7 post-fertilization human embryos contained a significant fraction of nuclei that had not undergone XCI by passages 20–24 under normoxic conditions based on the nuclear exclusion assay. Although it is difficult to relate hESCs to any stage of development, our data would lend strong support to the theory that hESCs and EpiSCs are not derived from an equivalent developmental stage using XCI and embryo morphology as an indicator. Instead, our data strongly support the hypothesis that XCI of hESCs is driven by *in vitro* culture, and that the timing of XCI after hESC derivation and the accumulation of XIST-independent class III nuclei is line-dependent.

In order to address the stability of class I, II and III nuclei, we cryopreserved the four female hESC lines at a time when the proportion of class I nuclei were >50% (UCLA1),

>70% (UCLA5) and >90% (UCLA3 and UCLA4). Our data demonstrate that unlike continuous culture from the point of derivation where class I nuclei are relatively stable up to passage 24, a single cryopreservation event followed by thawing and re-analysis again at passages 20–24 results in conversion or selection of class III nuclei in three out of four hESC lines. These data illustrate that a given hESC line can significantly change after a major event such as cryopreservation. From a practical perspective, our data indicate that sharing hESC lines between laboratories or initiating new experiments from cryopreserved stocks does not guarantee preservation of class I or II nuclei. The subline experiment using HSF-6 also indicates that expanding hESCs from single cells in the presence of ROCK inhibitor promotes the class III state. However, given that the parental line also progressed to 100% class III during the same time frame suggests that increased 'fitness' of class III cells resulting in outcompetition cannot be the sole cause for line progression to class III. Instead, our data argue that a combination of increased survival and epigenetic progression from class II to class III is responsible for increasing proportions of class III nuclei in a given hESC line with time.

One of the critical parameters in our study was the obvious heterogeneity at a single cell level within and between independently derived hESC lines with regard to the proportion of class I, II and III nuclear states. Under normoxic conditions, this epigenetic heterogeneity is ultimately resolved to an apparent irreversible class III XIST-independent state. In our studies, B and D were beneficial for improving the odds of retaining class I nuclei from new hESC derivations over sequential passages, but could not completely prevent the emergence of increasing proportions of class III nuclei with continuous culture post-derivation. This was further illustrated in the two HSF-6 sublines, where only 30% of nuclei were reprogrammed to class I, and the majority still progressed to class III. Why specific class II nuclei are more susceptible to B and B + D reprogramming is unclear from the current study, but suggests that within the class II population there is additional heterogeneity. Single-cell heterogeneity is a feature of hESC culture and is proposed to represent a stable continuum of cell states (36). Together, our data demonstrate that the effect of B and D are line-dependent, and we propose that this is due not to the stochastic effects of the chemicals, but instead to the proportion of class I, II and III nuclei at the time when the chemicals are first introduced. Put simply, the more class II and III nuclei in a given culture, the less effective the chemical treatment for acquiring or retaining class I.

Maintaining class I nuclei in the self-renewing state is critical for studies that involve examining mechanisms of XCI as well as X-linked diseases. However, there is evidence that class III cells differentiate poorly as EBs (17), and after extensive passaging, class III cells exhibit compromised response to BMP4 in adherent culture and an inability to differentiate into trophoblast (18). These studies have led to the hypothesis that cells in the class III state are less capable of differentiation and possibly no longer pluripotent in teratoma assays. Here, we show unequivocally that hESC lines composed of 100% class III nuclei are fully capable of losing OCT4 protein during differentiation *in vitro*, and differentiate as teratomas *in vivo*, thereby refuting the hypothesis that class III nuclei do not differentiate and are not pluripotent. It should be noted that the teratoma assay does not capture the nuances of lineage-directed *in vitro* differentiation where line-specific differences have been observed (37). In the current study, we do not know whether class III nuclei *in vitro* exhibit preference towards certain lineages or cell types relative to class I or II and this will be critical to analyze in future studies. This is particularly important given that *in vitro* differentiation is the clinically relevant starting point to cell therapy.

Prior to the current study, three independent methods had been developed to reverse or prevent XCI in hESCs. For example, derivation and maintenance in hypoxia improves the odds of retaining class I nuclei relative to normoxic conditions but cannot act to reprogram XCI cells to an active state (26). Although we did not evaluate hypoxia in our studies, our work does demonstrate that normoxia is compatible with the survival and self-renewal of class I nuclei for at least 20 passages without cryopreservation. Media supplementation with B has also been used previously to induce loss of *XIST* from H9 hESCs (28). Our data support a role for B in reprogramming class II nuclei to a class I state across multiple lines, although having no effect on class III. In more recent studies, hESCs can be reprogrammed to a naïve state by ectopic expression of *Oct4*, *Klf4* and *Klf2* and by growth in media used to culture murine ESCs (27). This strategy facilitates the recovery of cells that are capable of undergoing random XCI upon lineage differentiation. However, stable expression of transgenes is not relevant for generating clinically relevant cell types.

Although B and D supplementation demonstrates proof of principle that hESC nuclei in normoxic conditions can be maintained in the class I state, our microarray analysis indicated that B and D activity is not restricted to the X chromosome with the identification of more than 100 autosomal genes that are also differentially expressed in treated cultures. Gene ontology analysis did not reveal enrichment in any specific functional group. However, it did not escape our notice that one of the most significantly up-regulated gene was the imprinted gene H19, which was increased 36-fold with B + D treatment. Loss of imprinting has been associated with tumorigenicity (38). Furthermore, evidence exists that up-regulation of *H19* is associated with human hepatocellular carcinoma (39,40). Although we do not know the functional consequence of *H19* up-regulation on hESC biology, the fact that B + D caused gene expression changes genome-wide including an imprinted locus would possibly argue against the use of B + D in routine hESC culture as a strategy for sustaining the class I state.

In summary, our data highlight the importance of maintaining hESC derivation efforts. Gold standard hESC lines should be the benchmark for human pluripotent stem cell research and we have shown this is achievable by preventing and reversing epigenetic progression of a major *in vitro* artifact. Developing new experimental approaches aimed at sustaining human pluripotent nuclei in an epigenetic state closer in identity to the days 6–7 human blastocyst is to work towards a more robust gold standard.

MATERIALS AND METHODS

Human ESC derivation

Embryos from couples who had completed the IVF treatment were donated under informed consent approved by the UCLA Embryonic Stem Cell Research Oversight (ESCRO) Committee and the Institutional Review Boards (IRB). Cryopreserved embryos ranging from the 2PN to blastocyst stage were used to derive the new hESC lines reported here. Cleavage stage and younger embryos were thawed using THAW-KIT1 (Vitrolife) according to the manufacturer's instructions and cultured until day 3 in Quinn's Advantage Protein Plus Cleavage medium (SAGE Media) and then transferred to Quinn's Advantage Protein Plus Blastocyst medium (SAGE Media) until blastocyst formation. Frozen blastocysts were thawed using Blastocyst Thaw Media Kit (Irvine Scientific) and cultured overnight in Global medium (Life Global) supplemented with 10% human serum albumin (Life Global) or thawed in G-ThawKitBlast (Vitrolife) supplemented with 10% serum substitute supplement (Irvine Scientific) and cultured overnight in Quinn's Advantage Blastocyst medium (SAGE Media). All embryos were incubated at 37°C, 5% O_2 and 6.2% CO_2. Images of the embryos used to derive the six new hESC lines are shown in Supplementary Material, Figure S5. Only UCLA5 was derived from an embryo frozen at the 2PN stage. All other UCLA lines were derived from frozen blastocysts. At the time of hESC derivation, the zona-pellucida was removed using Tyrode's acid (Irvine Scientific) at room temperature (RT) for 2–4 min and then washed three times in blastocyst media. All embryos except UCLA4 were transferred directly onto γ-irradiated mouse embryonic fibroblasts and either manually cut with a splitting blade (Bioniche Animal Health) to separate the ICM from the surrounding trophoblasts or left intact. UCLA4 was subjected to further immunosurgery as previously described by Lavon *et al*. (41), before being plated onto MEFs. The embryos were plated onto feeders in 37°C incubators in the presence of 5% CO_2, in derivation media consisting of 80% DMEM/F-12 (Gibco), 20% knockout serum replacement (Gibco), 2 mM GlutaMAX-I, 1% non-essential amino acids, 50 U/ml penicillin and 50 μg/ml streptomycin (Invitrogen), 0.1 mM 2-mercaptoethanol (Sigma) and 30 ng/ml bFGF (Peprotech). After ∼10–14 days, half of the initial colony was manually split using a fire-polished pulled glass pipet and transferred onto a fresh layer of feeder cells. Manual passaging was carried out for several passages and then enzymatically using collagenase type IV 1 m/ml (Gibco). After about five passages, bFGF concentrations were reduced to 10 ng/ml using the same media formulation and 5%CO_2/37°C incubators as described above.

hESC culture and differentiation of established hESC lines

The hESC, HSF-6 (UCO6, 46XX) and H9 (WA09, 46XX) were cultured on MEFs as previously described (42). hESCs were cultured in the presence of 0.2 mM sodium butyrate (Sigma) and 0.1 μM DZNep. General differentiation was performed on growth factor-reduced matrigel (BD Biosciences)-treated cover slips. Differentiation media included DMEM/F12 (Gibco BRL) supplemented with 20% lot-tested fetal bovine serum (FBS) (Hyclone), 0.1 mM non-essential amino acids (Gibco BRL), 0.1 mM β-mercaptoethanol (Gibco BRL) and 1 mM L-glutamine (Gibco BRL). hESCs were growing on cover slips with MEFs. The cover slips were previously treated for 2 h with concentrated HCl and washed overnight. Experiments were conducted with prior approval from the UCLA Embryonic Stem Cell Research Oversight Committee.

Generating sublines from hESCs

Sublines of hESC HSF-6 and H9 were generated by colony-picking using an inverted microscope, or as single cells adopting previously described methods with some changes (43). A single cell suspension was obtained using TrypLE (Gibco,12605). The cells were mechanically resuspended, and clumps removed by filtration through 0.4 μm filter (BD Falcon). Ten cells were plated into one well of a 96-well plate containing MEFs in the presence of 10 μM of the ROCK inhibitor Y-27632. Only wells containing single colonies were transferred by picking, with future passages using collagenase type IV.

Histone extraction

Histone extraction was performed as previously described, with some changes (44). Briefly, nuclear extracts were prepared from 5×10^6 cells/ml hESC. The cells were resuspended in 1.0 ml of chilled hypotonic lysis buffer (10 mM Tris–HCl, pH 8.0, 1 mM KCl, 1.5 mM $MgCl_2$, 0.34 M sucrose, 10% glycerol and 1 μM DTT). Protease inhibitor (Roche, Cat. No.1697 498) and Triton X-100 to a final concentration of 0.1% were added. The incubation was performed at 4°C for 30 min with rotation. The nuclear pellet was resuspended with 0.5 ml of nuclear extraction buffer (0.2 N H_2SO_4, 10% glycerol and 1 mM, 2-mercaptoethanol) and incubated at 4°C overnight. Histones were precipitated with TCA (final concentration of 33%) at 4°C for 1 h. The histone pellet was washed with cold acetone and let dry for 30 min at RT. The dry pellets were resuspended with 4× NuPage buffer.

Western analysis of histone H3K4me3 and H3K27me3

Histone concentration was first measured by Novex 16% Tris–glycine gels (Invitrogen) stained with Coomassie Brilliant Blue (Invitrogen). Histones were electrophoresed through two gels, one stained with Coomassie Brilliant Blue to evaluate loading and the other transferred to Hybond ECL membrane (GE Healthcare). Immunoblotting was carried out with primary antibodies histone H3 (1:5000 dilution) and H3K4me3, H3K27me3 (1:2500 dilution) in 5% non-fat milk in TBST. Secondary antibody was donkey anti-rabbit IgGT-horseradish peroxidase (HRP) (GE Healthcare). Histones were detected using the ECL western blotting detection reagent (GE Healthcare).

Histone immunostaining

hESCs were grown 24–48 h on cover slips and fixed with 4% parafomaldehyde (electron microscopy science, EMS) in PBS for 15 min at RT. Cell permeabilization was performed with 0.5% ice-cold Triton X-100 for 15 min at RT. The cells were incubated with blocking solution (10% FBS, heat inactivated on 0.05% Tween on PBS) for 30 min at 37°C. The cover

slips were incubated with 1:50 dilution of H3K27me3 (Millipore 07-449) or H3K4me3 (Abcam ab8580-100), 4°C overnight. Secondary antibodies were anti-rabbit DyLight 595 (Jackson ImmunoResearch, 711−515−152). The nuclei were counterstained with DAPI and viewed with Leica DMR fluorescent microscope. Images were captured with the Quips mFISH software (Vysis).

Simultaneous immunolabeling of H3K4me3 and X chromosome FISH

After staining with H3K27me3, the cells were fixed again with 4% paraformaldehyde (EMS) in PBS, and incubated for 15 min at RT. X chromosome paint was carried out as previously described, with some modification (45). Cells were fixed again with methanol:acetic acid (3:1) at −20°C for 24 h, followed by dehydratation in 70, 90 and 100% ethanol for 3 min each. Cells were denaturated in 70% formamide/2× SSC at 85°C for 40 min, cooled down with cold 70% ethanol and dehydrated with 90 and 100% ethanol. A total volume of 12 μl of probe [3 μl of concentrated biotinylated probe and 9 μl of hybridization buffer (Cambio)] was used to detect the X chromosome by fluorescent *in situ* hybridization (DNA FISH) to ethanol-dehydrated cells according to the manufacturer's instruction. The probe was detected using a Biotin (FITC) Detection Kit (Cambio, 1089-KB-50). The nuclei were counterstained with DAPI and viewed with Leica DMR fluorescent microscope. Images were captured with the Quips mFISH software (Vysis).

Cot-1 RNA FISH and X chromosome FISH

Human fibroblasts were grown on cover slips for 24 h and fixed with 4% paraformaldehyde/PBS (EMS) for 15 min. Permiabilization was carried out with 0.5% Triton-100/PBS for 10 min. Cot-1 probe was labeled by random priming using Prime-It Fluor Kit (Stratagene) and Chroma Tide Alexa Fluor 594-5-dUTP (Invitrogen). The incorporation was extended to 60 min. The unincorporated nucleotides were removed by QIAquick PCR purification column (Qiagen). An amount of 3 μl of the probe was used and the hybridization was carried out as previously described (46). After Cot1 hybridization, X chromosome DNA FISH was performed using Human IDetect FISH probes as described below. The samples were refixed with 4% paraformaldehyde/PBS for 10 min and transferred to methanol acetic acid (3:1 v/v) for 24 h. The samples were denatured in 70% formamide/2× SSC at 85°C for 35 min and 5 μl of the probe was used for hybridization. The nuclei were counterstained with DAPI and viewed with Leica DMR fluorescent microscope. Images were captured with the Quips mFISH software (Vysis).

XIST RNA FISH

Human fibroblasts or hESCs were grown on cover slips for 24 h and then fixed in 4% formaldehyde for 15 min at RT. The cells were permeabilized in PBS containing 0.5% Triton-X for 5 min on ice and washed in PBS and 2× SSC. RNA FISH hybridization was carried out as previously described (47). The *XIST* probe was labeled by nick translation with biotin-16-dUTP. After overnight hybridization at 37°C, post-hybridization washes were done as previously described (Spector and Goldman 1998). The probe was detected using Biotin (FITC) Detection Kit (Cambio, 1089-KB-50). The nuclei were counterstained with DAPI and viewed with the Leica DMR fluorescent microscope. Images were captured with the Quips mFISH software (Vysis).

Three-color FISH

Fibroblasts were grown in DMEM supplemented with 10% FBS, L-glutamine, non-essential amino acids and penicillin–streptomycin. Cells were grown on gelatinized cover slips and fixed in 4% PFA in 1× PBS for 10 min at RT. Cells were permeabilized by incubation with 1× PBS with 0.2% Tween-20 (PB/Tween) and then incubated overnight in 70% ethanol at 4°C. The following day, cells were sequentially extracted to 100% ethanol and hybridized to double-stranded DNA probes labeled with Alexa 488 dUTP (Utx), Alexa 546 dCTP (Atrx) and Alexa 647 dCTP (Xist) for 48 h. Cover slips were washed in SSC and slides were mounted in Aquapolymount. Interphase nuclei were counted in at least five colonies per human cell line and the sum were tabulated and shown in the graph.

Microarray

Total RNA was extracted from HSF-6 (8) C, HSF-6 (8) B + D and HSF-6 (s9) using RNeasy RNA extraction columns (Qiagen). Prior to hybridization, RNA was labeled using FL-Ovation cDNA Biotin Module V2 (Affymetrix). Labeled RNA was hybridized to the Affymetrix Human Genome U133 plus 2.0 arrays (Affymetrix) using standard conditions. Three biological replicates were analyzed for each. Differentially expressed genes between groups were selected at $\geq$1.5-fold and $P < 0.001$ using the D-chip analysis software. The data discussed in this publication have been deposited in NCBI's Gene Expression Omnibus and are accessible through GEO Series accession number GSE33864 (http://www.ncbi.nlm.nih.gov/geo/query/acc.cgi?acc=GSE33864).

Flow cytometry

Adherent cells were dissociated with TrypLE (Invitrogen) at 37°C for 5 min. Single cells were resuspended in PBS with 1% bovine serum albumin (Sigma) and co-stained for TRA-1-81 (eBiosciences, 1:200) and APC-conjugated SSEA4 (R&D, 1:100) on ice for 20 min followed by a wash for 5 min. Indirect labeling of TRA-1-81 was performed with FITC-conjugated goat anti-mouse IgM (1:500) (Jackson ImmunoResearch).

Generation of teratomas

Surgery was performed following Institutional Approval for Appropriate Care and Use of Laboratory Animals by the UCLA Institutional Animal Care and Use Committee [Chancellor's Animal Research Committee (ARC)] (Animal Welfare Assurance number A3196-01). Briefly, for testicular tumors, a single incision was made in the peritoneal cavity

and the testis was pulled through the incision site. Using a 27-gauge needle, hESCs [HSF-6, HSF-6 sublines (S7, S8, S9), H9, H9 sublines (7, 8, 9), UCLA1, UCLA2, UCLA3, UCLA4, UCLA5, UCLA6] in a volume of 50 ml of 0.5× Matrigel (BD) were transplanted into the testis of adult SCID mice. Six weeks after surgery, mice were euthanized and the tumors removed for histology. Tumors were fixed in 4% paraformaldehyde for at least 24 h at RT. Tissue was embedded in paraffin and 5 μm sections were cut for analysis. Sections were stained with hematoxylin and eosin for histology.

Karyotype

G-banded karyotyping was performed by Cell Line Genetics (http://www.clgenetics.com) (Madison, WI, USA). Cells were shipped overnight in ESC media as live cells, and Cell Line Genetics subsequently performed metaphase spreads and Gimsea staining before counting 20 metaphases for each cell line to determine karyotype.

SUPPLEMENTARY MATERIAL

Supplementary Material is available at *HMG* online.

ACKNOWLEDGEMENTS

The authors would like to acknowledge Sohelia Azghadiand Jinghua Tang for technical assistance, Anne Lindgren for teratoma formation, and Victor E. Marquez at the National Cancer Institute, Frederick, MA, USA, for supplying DZNep. We would also like to acknowledge Steven Peckman of the UCLA-BSCRC for ensuring high-quality documentation and institutional oversight and review of our work with human embryos and derivation of new hESC lines.

Conflict of Interest statement. The authors declare that they have no competing interests.

FUNDING

This work was supported by P01 funds from the NIH/NIGMS (P01 P01GM081621), and funds from the UCLA Eli and Edythe Broad Center of Regenerative Medicine and Stem Cell Research (UCLA-BSCRC). The derivation and characterization of hESC lines UCLA1-6 was supported exclusively by a New Cell Line Award from CIRM and the UCLA-BSCRC (A.T.C.), and not funding from the NIH.

REFERENCES

1. Thomson, J.A., Itskovitz-Eldor, J., Shapiro, S.S., Waknitz, M.A., Swiergiel, J.J., Marshall, V.S. and Jones, J.M. (1998) Embryonic stem cell lines derived from human blastocysts. *Science*, **282**, 1145–1147.
2. Takahashi, K., Tanabe, K., Ohnuki, M., Narita, M., Ichisaka, T., Tomoda, K. and Yamanaka, S. (2007) Induction of pluripotent stem cells from adult human fibroblasts by defined factors. *Cell*, **131**, 861–872.
3. Yu, J., Vodyanik, M.A., Smuga-Otto, K., Antosiewicz-Bourget, J., Frane, J.L., Tian, S., Nie, J., Jonsdottir, G.A., Ruotti, V., Stewart, R. *et al.* Induced pluripotent stem cell lines derived from human somatic cells. *Science*, **318**, 1917–1920.
4. Park, I.H., Zhao, R., West, J.A., Yabuuchi, A., Huo, H., Ince, T.A., Lerou, P.H., Lensch, M.W. and Daley, G.Q. (2008) Reprogramming of human somatic cells to pluripotency with defined factors. *Nature*, **451**, 141–146.
5. Lowry, W.E., Richter, L., Yachechko, R., Pyle, A.D., Tchieu, J., Sridharan, R., Clark, A.T. and Plath, K. (2008) Generation of human induced pluripotent stem cells from dermal fibroblasts. *Proc. Natl Acad. Sci. USA*, **105**, 2883–2888.
6. Zhu, S., Li, W., Zhou, H., Wei, W., Ambasudhan, R., Lin, T., Kim, J., Zhang, K. and Ding, S. (2008) Reprogramming of human primary somatic cells by OCT4 and chemical compounds. *Cell Stem Cell*, **7**, 651–655.
7. Huangfu, D., Osafune, K., Maehr, R., Guo, W., Eijkelenboom, A., Chen, S., Muhlestein, W. and Melton, D.A. (2008) Induction of pluripotent stem cells from primary human fibroblasts with only Oct4 and Sox2. *Nat. Biotech.*, **26**, 1269–1275.
8. Zhao, T., Zhang, Z.N., Rong, Z. and Xu, Y. (2011) Immunogenicity of induced pluripotent stem cells. *Nature*, **474**, 212–215.
9. Chin, M.H., Mason, M.J., Xie, W., Volinia, S., Singer, M., Peterson, C., Ambartsumyan, G., Aimiuwu, O., Richter, L., Zhang, J. *et al.* (2009) Induced pluripotent stem cells and embryonic stem cells are distinguished by gene expression signatures. *Cell Stem Cell*, **5**, 111–123.
10. Doi, A., Park, I.H., Wen, B., Murakami, P., Aryee, M.J., Irizarry, R., Herb, B., Ladd-Acosta, C., Rho, J., Loewer, S. *et al.* (2009) Differential methylation of tissue- and cancer-specific CpG island shores distinguishes human induced pluripotent stem cells, embryonic stem cells and fibroblasts. *Nat. Genet.*, **41**, 350–1353.
11. Guenther, M.G., Frampton, G.M., Soldner, F., Hockemeyer, D., Mitalipova, M., Jaenisch, R. and Young, R.A. (2010) Chromatin structure and gene expression programs of human embryonic and induced pluripotent stem cells. *Cell Stem Cell*, **7**, 249–257.
12. Lister, R., Pelizzola, M., Dowen, R.H., Hawkins, R.D., Hon, G., Tonti-Filippini, J., Nery, J.R., Lee, L., Ye, Z., Ngo, Q.M. *et al.* (2009) Human DNA methylomes at base resolution show widespread epigenomic differences. *Nature*, **462**, 315–322.
13. Laurent, L.C., Ulitsky, I., Slavin, I., Tran, H., Schork, A., Morey, R., Lynch, C., Harness, J.V., Lee, S., Barrero, M.J. *et al.* (2011) Dynamic changes in the copy number of pluripotency and cell proliferation genes in human ESCs and iPSCs during reprogramming and time in culture. *Cell Stem Cell*, **8**, 106–118.
14. Bock, C., Kiskinis, E., Verstappen, G., Gu, H., Boulting, G., Smith, Z.D., Ziller, M., Croft, G.F., Amoroso, M.W., Oakley, D.H. *et al.* (2011) Reference maps of human ES and iPS cell variation enable high-throughput characterization of pluripotent cell lines. *Cell*, **144**, 439–452.
15. Okamoto, I., Patrat, C., Thépot, D., Peynot, N., Fauque, P., Daniel, N., Diabangouaya, P., Wolf, J.P., Renard, J.P., Duranthon, V. *et al.* (2011) Eutherian mammals use diverse strategies to initiate X-chromosome inactivation during development. *Nature*, **472**, 370–374.
16. Shen, Y., Matsuno, Y., Fouse, S.D., Rao, N., Root, S., Xu, R., Pellegrini, M., Riggs, A.D. and Fan, G. (2008) X-inactivation in female human embryonic stem cells is in a nonrandom pattern and prone to epigenetic alterations. *Proc. Natl Acad. Sci. USA*, **105**, 4709–4714.
17. Silva, S.S., Rowntree, R.K., Mekhoubad, S. and Lee, J.T. (2008) X-chromosome inactivation and epigenetic fluidity in human embryonic stem cells. *Proc. Natl Acad. of Sci. USA*, **105**, 4820–4825.
18. Tanasijevic, B., Dai, B., Ezashi, T., Livingston, K., Roberts, R.M. and Rasmussen, T.P. (2009) Progressive accumulation of epigenetic heterogeneity during human ES cell culture. *Epigenetics*, **4**, 330–338.
19. Dvash, T., Lavon, N. and Fan, G. (2010) Variations of X chromosome inactivation occur in early passages of female human embryonic stem cells. *PloS One*, **5**, e11330.
20. Marchetto, M.C., Carromeu, C., Acab, A., Yu, D., Yeo, G.W., Mu, Y., Chen, G., Gage, F.H. and Muotri, A.R. (2010) A model for neural development and treatment of Rett syndrome using human induced pluripotent stem cells. *Cell*, **143**, 527–539.
21. Tchieu, J., Kuoy, E., Chin, M.H., Trinh, H., Patterson, M., Sherman, S.P., Aimiuwu, O., Lindgren, A., Hakimian, S., Zack, J.A. *et al.* (2010) Female human iPSCs retain an inactive X chromosome. *Cell Stem Cell*, **7**, 329–342.
22. Pomp, O., Dreesen, O., Leong, D.F., Meller-Pomp, O., Tan, T.T., Zhou, F. and Colman, A. (2011) Unexpected X chromosome skewing during culture and reprogramming of human somatic cells can be alleviated by exogenous telomerase. *Cell Stem Cell*, **9**, 156–165.

23. Plath, K., Fang, J., Mlynarczyk-Evans, S.K., Cao, R., Worringer, K.A., Wang, H., de la Cruz, C.C., Otte, A.P., Panning, B. and Zhang, Y. (2003) Role of histone H3 lysine 27 methylation in X inactivation. *Science*, **300**, 131–135.
24. Zhao, J., Sun, B.K., Erwin, J.A., Song, J.J. and Lee, J.T. (2008) Polycomb proteins targeted by a short repeat RNA to the mouse X chromosome. *Science*, **322**, 750–756.
25. Pera, M.F. and Tam, P.P. (2010) Extrinsic regulation of pluripotent stem cells. *Nature*, **465**, 713–720.
26. Lengner, C.J., Gimelbrant, A.A., Erwin, J.A., Cheng, A.W., Guenther, M.G., Welstead, G.G., Alagappan, R., Frampton, G.M., Xu, P., Muffat, J. *et al.* (2010) Derivation of pre-X inactivation human embryonic stem cells under physiological oxygen concentrations. *Cell*, **141**, 872–883.
27. Hanna, J., Cheng, A.W., Saha, K., Kim, J., Lengner, C.J., Soldner, F., Cassady, J.P., Muffat, J., Carey, B.W. and Jaenisch, R. (2010) Human embryonic stem cells with biological and epigenetic characteristics similar to those of mouse ESCs. *Proc. Natl Acad. Sci. USA*, **107**, 9222–9227.
28. Ware, C.B., Wang, L., Mecham, B.H., Shen, L., Nelson, A.M., Bar, M., Lamba, D.A., Dauphin, D.S., Buckingham, B., Askari, B. *et al.* (2009) Histone deacetylase inhibition elicits an evolutionarily conserved self-renewal program in embryonic stem cells. *Cell Stem Cell*, **4**, 359–369.
29. Fiskus, W., Wang, Y., Sreekumar, A., Buckley, K.M., Shi, H., Jillella, A., Ustun, C., Rao, R., Fernandez, P., Chen, J. *et al.* (2009) Combined epigenetic therapy with the histone methyltransferase EZH2 inhibitor 3-deazaneplanocin A and the histone deacetylase inhibitor panobinostat against human AML cells. *Blood*, **114**, 2733–2743.
30. Musch, T., Oz, Y., Lyko, F. and Breiling, A. (2010) Nucleoside drugs induce cellular differentiation by caspase-dependent degradation of stem cell factors. *PloS One*, **5**, e10726.
31. Tan, J., Yang, X., Zhuang, L., Jiang, X., Chen, W., Lee, P.L., Karuturi, R.K., Tan, P.B., Liu, E.T. and Yu, Q. (2007) Pharmacologic disruption of polycomb-repressive complex 2-mediated gene repression selectively induces apoptosis in cancer cells. *Genes Dev.*, **21**, 1050–1063.
32. Miranda, T.B., Cortez, C.C., Yoo, C.B., Liang, G., Abe, M., Kelly, T.K., Marquez, V.E. and Jones, P.A. (2009) DZNep is a global histone methylation inhibitor that reactivates developmental genes not silenced by DNA methylation. *Mol. Can. Ther.*, **8**, 1579–1588.
33. Sustackova, G., Legartová, S., Kozubek, S., Stixová, L., Pacherník, J. and Bártová, E. (2011) Differentiation-independent fluctuation of pluripotency-related transcription factors and other epigenetic markers in embryonic stem cell colonies. *Stem Cells Dev*., [Epup ahead of print].
34. Brons, I., Smithers, L.E., Trotter, M.W., Rugg-Gunn, P., Sun, B., Chuva de Sousa Lopes, S.M., Howlett, S.K., Clarkson, A., Ahrlund-Richter, L., Pedersen, R.A. *et al.* (2007) Derivation of pluripotent epiblast stem cells from mammalian embryos. *Nature*, **448**, 191–195.
35. Tesar, P., Chenoweth, J.G., Brook, F.A., Davies, T.J., Evans, E.P., Mack, D.L., Gardner, R.L. and McKay, R.D. (2007) New cell lines from mouse epiblast share defining features with human embryonic stem cells. *Nature*, **448**, 196–199.
36. Hough, S.R., Laslett, A.L., Grimmond, S.B., Kolle, G. and Pera, M.F. (2009) A continuum of cell states spans pluripotency and lineage commitment in human embryonic stem cells. *PloS One*, **4**, e7708.
37. Kim, K., Doi, A., Wen, B., Ng, K., Zhao, R., Cahan, P., Kim, J., Aryee, M.J., Ji, H., Ehrlich, L.I. *et al.* (2010) Epigenetic memory in induced pluripotent stem cells. *Nature*, **467**, 285–290.
38. Bjornsson, H.T., Brown, L.J., Fallin, M.D., Rongione, M.A., Bibikova, M., Wickham, E., Fan, J.B. and Feinberg, A.P. (2007) Epigenetic specificity of loss of imprinting of the IGF2 gene in Wilms tumors. *J. Natl. Cancer Inst.*, **99**, 1270–1273.
39. Matouk, I.J., DeGroot, N., Mezan, S., Ayesh, S., Abu-lail, R., Hochberg, A. and Galun, E. (2007) The H19 non-coding RNA is essential for human tumor growth. *PloS One*, **2**, e845.
40. Ariel, I., Miao, H.Q., Ji, X.R., Schneider, T., Roll, D., de Groot, N., Hochberg, A. and Ayesh, S. (1998) Imprinted H19 oncofetal RNA is a candidate tumour marker for hepatocellular carcinoma. *Mol. Pathol.*, **51**, 21–25.
41. Lavon, N., Narwani, K., Golan-Lev, T., Buehler, N., Hill, D. and Benvenisty, N. (2008) Derivation of euploid human embryonic stem cells from aneuploid embryos. *Stem Cells*, **26**, 874–1882.
42. Clark, A.T., Bodnar, M.S., Fox, M., Rodriquez, R.T., Abeyta, M.J., Firpo, M.T. and Pera, R.A. (2004) Spontaneous differentiation of germ cells from human embryonic stem cells *in vitro*. *Hum. Mol. Genet.*, **13**, 727–739.
43. Pyle, A., Lock, F. and Donovan, P. (2006) Neurotrophins mediate human embryonic stem cell survival. *Nat. Biotechnol.*, **24**, 344–350.
44. Shechter, D., Dormann, H.L., Allis, C.D. and Hake, S.B. (2007) Extraction, purification and analysis of histones. *Nat. Protoc.*, **2**, 1445–1457.
45. Diaz-Perez, S.V., Ferguson, D.O., Wang, C., Csankovszki, G., Wang, C., Tsai, S.C., Dutta, D., Perez, V., Kim, S., Eller, C.D. *et al.* (2006) A deletion at the mouse Xist gene exposes trans-effects that alter the heterochromatin of the inactive X chromosome and the replication time and DNA stability of both X chromosomes. *Genetics*, **174**, 1115–1133.
46. Namekawa, S. and Lee, J. (2011) Detection of nascent RNA, single-copy DNA and protein localization by immunoFISH in mouse germ cells and preimplantation embryos. *Nat. Protoc.*, **6**, 270–280.
47. Spector, D. and Goldman, R. (1998) In Spector, D.L. and Goldman, R.D (eds), *Essentials from Cells: A Laboratory Manual*. Cold Spring Harbor Laboratory Press, Cold Spring Harbor, NY, pp. 114–117.